

Design, Fabrication, and Test of a Hydrothermal Reactor for Origin-of-Life Experiments

Randall E. Mielke,¹ Michael J. Russell,^{1,2} Philip R. Wilson,¹ Shawn E. McGlynn,^{1,2,*}
Max Coleman,^{1,2} Richard Kidd,¹ and Isik Kanik^{1,2}

Abstract

We describe a continuous high-pressure flow reactor designed to simulate the unforced convective interaction of hydrothermal solutions and ocean waters with submarine crust on early Earth—conditions appropriate to those that may have led to the onset of life. The experimental operating conditions are appropriate for investigating kinetic hydrothermal processes in the early history of any sizable wet, rocky planet. Beyond the description of the fabrication, we report an initial experiment that tested the design and investigated the feasibility of sulfide and silica dissolution in alkaline solution from iron sulfide and basaltic rock, and their possible subsequent transport as HS^- and $\text{H}_2\text{SiO}_4^{2-}$ in hot alkaline solutions. Delivery of hydrogen sulfide and dihydrogen silicate ions would have led to the precipitation of ferrous hydroxide, hydroxysilicates, and iron sulfides as integral mineral components of an off-ridge compartmentalized hydrothermal mound in the Hadean. Such a mound could, we contend, have acted as a natural chemical and electrochemical reactor and, ultimately, as the source of all biochemistry on our planet. In the event, we show that an average of $\sim 1 \text{ mM/kg}$ of both sulfide and silica were released throughout, though over 10 mM/kg of HS^- was recorded for ~ 100 minutes in the early stages of the experiment. This alkaline effluent from the reactor was injected into a reservoir of a simulacrum of ferrous iron-bearing “Hadean Ocean” water in an experiment that demonstrated the capacity of such fluids to generate hydrothermal chimneys and a variety of contiguous inorganic microgeode precipitates bearing disseminations of discrete metal sulfides. Comparable natural composite structures may have acted as hatcheries for emergent life in the Hadean. Key Words: Hydrothermal reactor—Hydrothermal mound—Hydrothermal chimneys—Geodes—Transition-metal sulfides—Hadean Ocean. *Astrobiology* 10, 799–810.

1. Introduction

ONE HYPOTHESIS for the origin of life posits that its prebiotic building components were synthesized within moderate temperature ($\leq 130^\circ\text{C}$) hydrothermal chimneys and mounds on the floor of the most ancient (Hadean) ocean before the unambiguous geological record began on Earth (Russell *et al.*, 1989). Mounds like these—precipitated where off-ridge alkaline, calcium-, silica-, sulfide-, and H_2 -bearing spring waters met with carbonic ocean water that contained ferrous iron and photo-oxidized iron colloids—would have acted as natural electrochemical flow reactors whereby hydrogen, derived through serpentinization, could reduce carbon oxides to produce simple organic molecules, driven by ambient redox and proton gradients

acting across inorganic precipitate membranes (Russell *et al.*, 1994; Russell and Martin, 2004; Nitschke and Russell, 2010, Fig. 6), notionally:



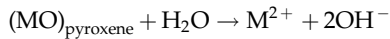
The catalytic pores in these ancient mounds are envisaged to consist of iron-nickel sulfide clusters and nanocrystals dosed with cobalt, molybdenum, and tungsten embedded in clays, amorphous silica, and carbonate. Such compartments have been considered to comprise the hatchery of life (Russell and Hall, 2006). The hydrothermal fluids that fed the mounds would have been rendered alkaline as ocean waters convected within the oceanic crust through the dissolution of calcium, along with a minor portion of the magnesium from komatiitic lavas or

¹Jet Propulsion Laboratory, California Institute of Technology, Pasadena, California.

²NASA Astrobiology Institute.

*Present address: Department of Chemistry and Biochemistry and the Astrobiology Biogeochemistry Research Center, Montana State University, Bozeman, Montana.

ultramafic crust, during serpentinization to produce soluble hydroxides (Russell *et al.*, 1989, 2010; Macleod *et al.*, 1994).



The conditions pertinent to the emergence of life, which we attempted to reproduce in this study, stand in strong contrast to the acidic hydrothermal fluids that likely were exhaled from ocean ridges and volcanoes and favored for biosynthesis by Corliss (1986) and Wächtershäuser (2006). Since the formulation of the alkaline hydrothermal scenario, a broadly comparable alkaline ($\text{pH} \leq 12.1$) hydrothermal system was discovered at the Lost City site in the North Atlantic 15 km west of the Mid-Atlantic Ridge at 30°N, above serpentinized peridotites (Kelley *et al.*, 2001, 2005; Martin *et al.*, 2008). Recorded temperatures of the effluent there reach ~94°C (Kelley *et al.*, 2005; Charlou *et al.*, 2010). Another submarine alkaline system ($\text{pH} \sim 10$), which consists mainly of clays and is fed largely with 11,000-year-old fresh water, was discovered exhaling from basaltic lavas in Eyjafjörður, northern Iceland, at temperatures up to 78°C (Marteinsson *et al.*, 2001; Gautason *et al.*, 2005; Hreiðar Þór Valtýsson, personal communication, 2010). The temperatures and pH values at Lost City and Eyjafjörður are comparable to some of those detected in certain subaerial springs in ophiolitic terrains (Barnes *et al.*, 1972; Neal and Stanger, 1984; Abrajano *et al.*, 1990; Fallick *et al.*, 1991). Given this information and considering the hydrogen isotopic results of Proskurowski *et al.* (2006) from Lost City, we deem the temperature of the fluids at the base of the open system hydrothermal cells that feed such submarine mounds to be thermostated around 130°C (Russell *et al.*, 2010). Though at odds with the interpretations of Foustoukos *et al.* (2008) and our own earlier estimates (Russell and Hall, 1997), we take this view with the presumption that above 130°C serpentine becomes too plastic—in the absence of magmatic intrusion—to force convection, which thereby renders portions of the crust impermeable to waters under hydrostatic pressure. In contrast to the assumption that the Lost City system is magma driven (Allen and Seyfried, 2004), we have argued, as have others, that the continual heating of the aqueous fluids is partly a result of the geothermal gradient, partly the downward migration of the base of the hydrothermal cell, and partly a result of exothermic reactions (Russell, 1978; Lowell and Rona, 2002; Kelley *et al.*, 2005; Ludwig *et al.*, 2005; Emmanuel and Berkowitz, 2006; Russell *et al.*, 2010). While such physical constraints are generally invariant between the Hadean and the present day, the same cannot be said for the chemistry in that, given the ambient oxygenated seawater and the waste products from populations of archaea and bacteria, along with differences in crustal mineralogy and structure, neither Lost City nor Eyjafjörður can be considered directly analogous to a lifeless Hadean hydrothermal system and its submarine springs.

Thus, because of these uncertainties there is a need to address the hypothesis in the laboratory in oxygen-free and sterile conditions. To this end and to test our expectations as to the effects of mixing a simulacrum of ancient carbonic ocean water with alkaline hydrothermal solution, we describe the design, fabrication, and operation of the hydrothermal reactor built to reproduce the relevant conditions on early Earth or any other wet and rocky world with a carbonic ocean, such as

Europa (Hand *et al.*, 2007, 2010; Vance *et al.*, 2007). Specifically, the reactor was built to (i) reproduce chemical interactions as hydrothermal waters flow in a conduit through rocks just beneath the ancient ocean floor at ~100 bar H_2 pressure and up to 130°C; (ii) assess the chemical interactions between the hydrothermal solution and carbonic ocean water that might give rise to a freshly precipitated carbonate-, silica-, and sulfide-bearing hydrothermal mound; and (iii) test the potential of such a hydrothermal system of synthesizing particular organic molecules, if any, through the hydrogenation of carbon oxides.

In this contribution, we describe the construction and testing of such a reactor and then report results of our first experiment, which addressed silica and sulfide dissolution from iron sulfides and basaltic rock wool in a representation of a Hadean Ocean crust (Fig. 1). While there is some geological evidence for the dissolution of sulfides in the ocean crust under non-equilibrium alkaline hydrothermal conditions (Delacour *et al.*, 2008), the absence of a rock record of early Earth and a lack of a modern example of sulfide delivery in

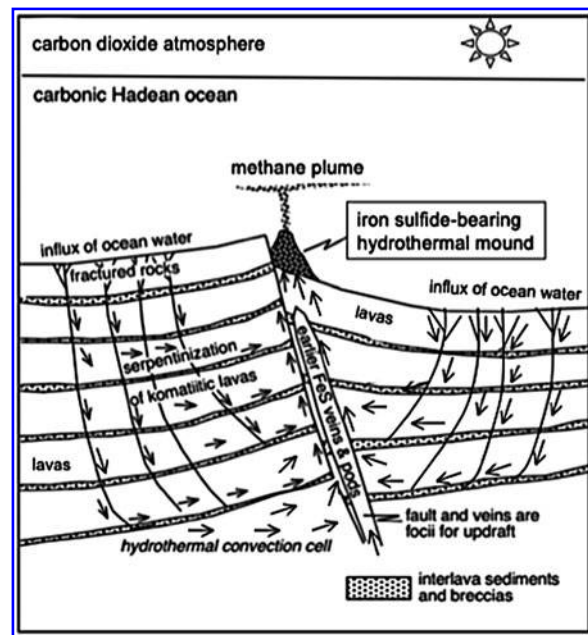


FIG. 1. A scenario for the emergence of life whereby the first organic building components are generated in a natural hydrothermal reactor (the iron sulfide-bearing mound figured here) produced over an unforced convection cell operating at hydrostatic pressure on the Hadean Ocean floor (*cf.* Figs. 8 and 9). A reactor simulating these conditions is described in the text and shown in Fig. 2. Key to catalysis and electron transfer in the natural reactor is a supply of hydrogen sulfide anion (HS^- , dissolved from the iron sulfides beneath) to react with the ferrous (and minor ferric) iron in the early ocean, a concern of the test experiment. Occasional iron sulfide veins and pods within ocean floor sequences of komatiitic lavas would have been a source of soluble hydrogen sulfide ion (*e.g.*, Leshner and Stone, 1997), and gabbros, cherts, or quartz veins as the source of silica (Barnes *et al.*, 1972; Fallick *et al.*, 1991). Serpentinization is the process of hydration, carbonation, and oxidation of komatiites and other mineralogically comparable rocks thought to be an initial requirement for life's emergence (Russell *et al.*, 1989).

alkaline springs dictated that this would be our first experimental test. Indeed, the known chambered alkaline hydrothermal precipitate mounds at Lost City consist mainly of carbonates with minor brucite (Kelley *et al.*, 2001), whereas at Eyjafjardur, North Iceland, they are composed of sepiolite (Marteinsson *et al.*, 2001). Sepiolites mixed with poorly crystalline Fe-Mn hydroxides at the Owen fracture zone (a transform fault) in the Indian Ocean at $\sim 12^\circ\text{N}$, $\sim 58^\circ\text{E}$, also appear to be the vestiges of precipitates from alkaline springs (Bonatti *et al.*, 1983). This (almost) complete lack of sulfide in modern alkaline springs is a potential threat to the “alkaline hydrothermal hypothesis,” as we have argued that metal sulfides, as constituents of inorganic membranes, are central to redox catalysis and the transfer of protons from the ocean to the porous interiors required of chemiosmosis (Russell *et al.*, 1994; Martin and Russell, 2007; Nitschke and Russell, 2009). Silica activities too are generally low in fluids that interact with ultramafic rock (Palandri and Reed, 2004). Nevertheless, silica veins and subaerial precipitates are common in serpentinized terrains, where gabbros, cherts, or other siliceous rocks occur in the footwall (Barnes *et al.*, 1972; Fallick *et al.*, 1991; Zedef *et al.*, 2000). Moreover, the submarine alkaline springs emanating from basalt rather than ultramafic rock at Eyjafjardur contain $\sim 1.6\text{ mM/L}$ SiO_2 (Marteinsson *et al.*, 2001), and in any case silica concentrations in the Hadean Ocean could have reached 5 mM/L (Knauth and Lowe, 2003).

In the origin-of-life model considered here, the silica and hydrogen sulfide anions are expected to bring about the precipitation of catalytic sulfide-bearing (cobalt- and tungsten-doped- $\text{FeS} > \text{Fe}(\text{Ni})\text{S} \gg \text{NiFe}_5\text{S}_8 \gg \text{MoS}_2$) compartments through interaction with “oceanic” iron ($\text{Fe}^{2+} \gg \text{Fe}^{\text{III}}$), nickel, and cobalt (Fig. 1). These transition metals, dissolved as clusters or occurring as nanoparticles in the early oxygen-free carbonic ocean, were ultimately derived from much hotter ($360\text{--}400^\circ\text{C}$) acidic submarine springs (Douville *et al.*, 2002; Kump and Seyfried, 2005). At the pressures and moderate temperatures indicated by the model, the alkaline fluids also had the theoretical propensity to dissolve calcium and minor magnesium from silicates (Palandri and Reed, 2004), and silica from cherts or quartz veins (Kehew, 2001). Thus, the effluent from this first experiment might be expected to produce chimneys or compartments, or both, on injection into a ferrous iron-bearing solution representing the Hadean Ocean. Such inorganic compartments are expected to hold a redox and proton tension between simulacra of the hydrogen-bearing alkaline hydrothermal interior of the mound and the mildly acidic carbonic ocean bathing the exterior. Oxidized entities apart from CO_2 in the Hadean Ocean would be phosphate, nitric oxides and nitrate, and photochemically generated ferric iron particles (Braterman *et al.*, 1983; Yamagata *et al.*, 1991; Martin *et al.*, 2007). In the event, the reactor operated to plan; some sulfide, silica, and calcium were dissolved in the solution, which, on exhalation into the ferrous solution, did produce sturdy chimneys and compartments dosed with iron sulfide and ferrous hydroxide.

2. Material and Methods

2.1. Reactor design and construction

Two 3.8 L, pressure-tested 316 electro-polished alloy stainless steel (316epSS) cylinders were employed as solution reservoirs, one for the hydrothermal solution and one for the

simulated Hadean Ocean. Heating coils allow the fluids to be subjected to temperatures of up to 140°C . Each of the two reservoirs has two access ports, one at the top for pumping out headspace gases and for the introduction of liquids, and the other at the base so that the gases may be bubbled through the solution to ensure full gas/water exchange prior to each run. The vessels are connected through high-pressure 316SS non-return and two-way ball valves to the lagged central tee connector to the reactor (Fig. 2). The reactor itself was fabricated, assembled, and operated in the Jet Propulsion Laboratories, California Institute of Technology. The requirements for high-pressure hydrogen (~ 100 bars), weldable material, and a minimum of catalytic activity dictated the use of a chrome steel barrel with an electro-polished chromium oxide interior for the reactor. For safety, it was built and tested to tolerate at least 400 atmospheres. It is 508.0 mm long and has an outer diameter of 25.4 mm and an internal diameter of 19.1 mm. The feed to the reactor from both the hydrothermal vessel and the ocean vessel is driven by hydrogen overpressure and controlled by 316SS non-return ball valves and high-pressure needle valves. A screw connection is placed at the T-joint to allow retrieval of the packing material and catalyst for analysis and also for the cleaning of the barrel. Heating of the vessels and reactor is by rheostatically controlled thermoelectric coils, and the temperature is measured electronically by DT-670D-SD temperature sensors. At this central location, the two fluids may be alternately introduced to the reactor barrel that stands slanted 10° from the vertical to simulate the hydrothermal conduit and the hydrothermal mound (Figs. 1 and 2).

Before operations, the reactor was flushed with 4% HCl/4% HNO_3 solution (15 min) followed by three Milli-Q ($18.2\text{ M}\Omega$) water washes (15 min each), and baked out at 300°C under helium. The reactor was then packed with basaltic rock wool (or crysotile asbestos if health and safety conditions allow), which acts as a crustal (or mantle) rock analogue and support for crushed sulfide minerals or as a substrate for freshly precipitated iron (nickel) sulfide catalyst. Temperatures can be controlled up to 140°C over the lower 258 mm—the remaining 254 mm simulates the natural cooling of hydrothermal fluids as they interface colder Hadean Ocean waters at the base of the mound. To relieve pressure, the reactor feeds into 3 m long, 1.59 mm (1/16 inch) 316SS tubing and terminates in a three-way valve for sample distribution through 1 m of 0.075 mm silica capillary lines. The capillary lines are fed into helium-purged, acid-washed 20 mL or 120 mL crimp-top vials. The effluent delivery rate approximates $3\ \mu\text{L/s}$.

2.2. Preparation of solutions

For the first hydrothermal vent experiment, 3.5 L of both ocean water simulant and the hydrothermal solution (derived from the same ocean water simulant) were charged with sodium chloride at 35 g/L to mimic present-day ocean and alkaline hydrothermal solutions. This value was chosen on the assumption that the Hadean Ocean was largely sourced from high-temperature springs exhaling from ultramafic crust (Wetzel and Shock, 2000). It is noteworthy that there is little contrast between the sodium content of hydrothermal fluids at Lost City and that of the ocean (Charlou

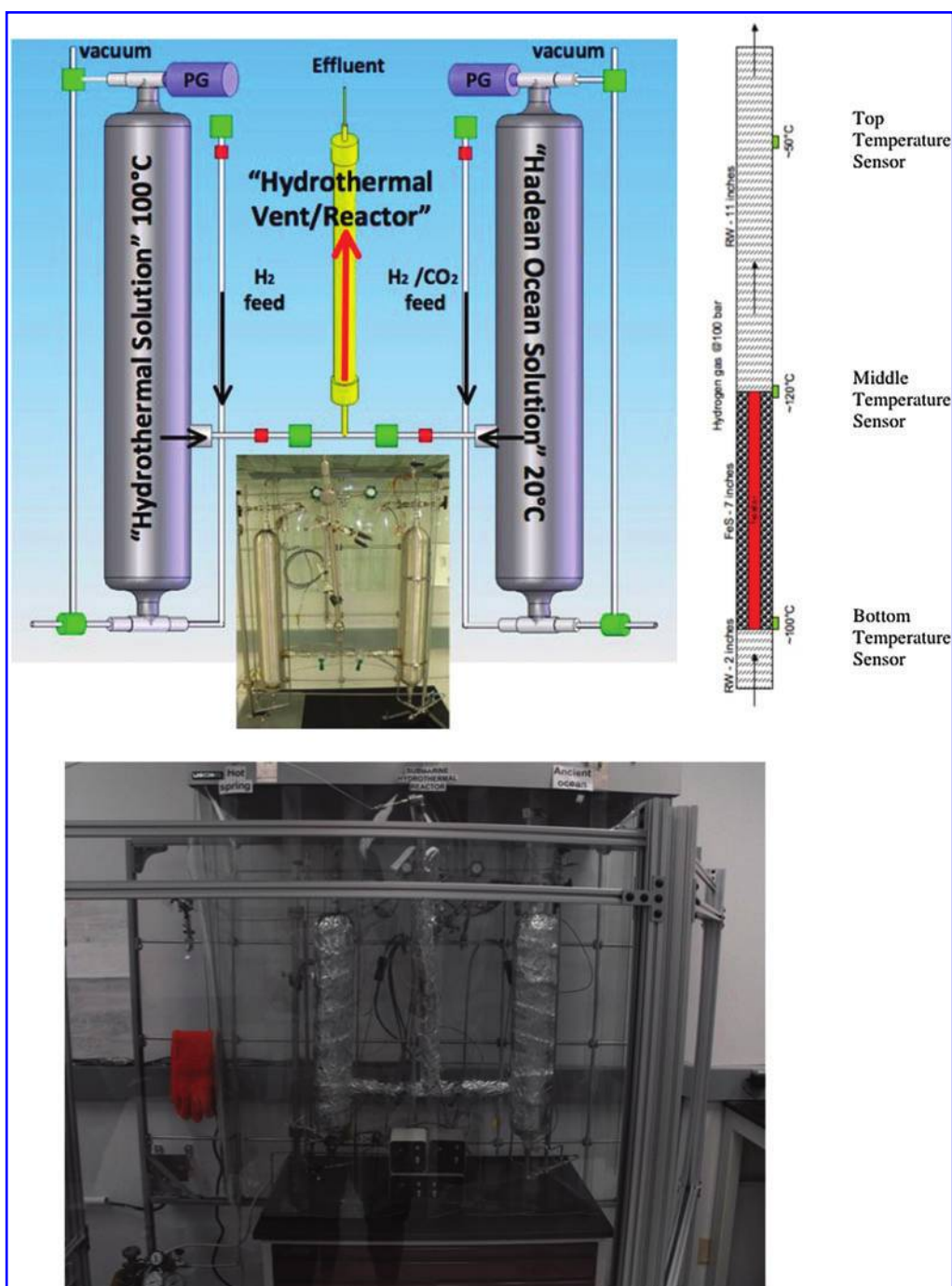


FIG. 2. Top: CAD drawing of the reactor design with inset photograph of the reactor before lagging with thermoelectric coil. Two-way or three-way valves are shown in green, and non-return ball valves are in red. Gasses are purged into solutions through the bottom port to ensure adequate gas/solution interface time. The reactor on the right illustrates placement of temperature sensors on the external reactor surface and the distribution inside the reactor of iron sulfide (FeS) and rock wool. Bottom: the lagged system. PG, pressure gauge. Color images available online at www.liebertonline.com/ast.

et al., 2010). In addition, 10 mM/L of sodium bicarbonate was introduced to the hydrothermal solution, which was adjusted with ~1 mL of dilute sodium hydroxide to pH 12.0—comparable to peak pH in submarine serpentinite pore waters and the Lost City effluent (Macleod *et al.*, 1994; Salisbury, 2002; Charlou *et al.*, 2010). The ocean solution was prepared at pH 5.3, and ammonium bicarbonate was added to the level of 0.5 mM/L. This solution was then readjusted

to pH 5.3 with ~1 mL dilute hydrochloric acid to maintain a final volume of 3.5 L (Macleod *et al.*, 1994).

The two electro-polished stainless steel cylinders, previously baked out and washed with deionized water, were filled with 3.5 L of each of the solutions. Prior to the experimental run, helium was bubbled through the lower ports into the filled cylinders at 100 psi and ambient temperatures for a 15 min flush to remove any last vestiges of oxygen and

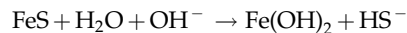
nitrogen. Three consecutive flushings and head-space pumping removed all air from fluids and in head space prior to the introduction of hydrogen gas. Following the final pumping sequence, hydrogen was introduced through the bottom of both reservoirs at a pressure of 1500 psi (~ 100 bar) equivalent to 160 mM/L of hydrogen (Wiebe and Gaddy, 1934). The base of the reactor was packed with 50 mm of basalt rock wool (Minwood 1200, Industrial Insulation Group, Al, USA). In atomic percentage it comprises SiO₂ 51.7; CaO 17.2; MgO 16.2; Al₂O₃ 9.0; FeO 2.5; Na₂O 2.7; K₂O <0.1; P₂O₅ 0.5 (ESEM-EDAX), in the compositional range of a calc-alkaline basalt. The next 180 mm of the reactor (above the rock wool) were packed with reagent-grade iron monosulfide (FeS) (Argos Organics, Geel, Belgium; crushed to ~ 1 mm fragments to increase reactive surface area and promote mineral/water interaction without clogging the effluent capillary lines). The remaining (upper) 280 mm was also packed with basalt rock wool. (The calcium content of the rock wool is high compared to mafic rock; however, health and safety decreed that chrysotile, our preferred crustal simulant but a carcinogen, not be used.) The reactor barrel was heated to a maximum of 130°C, with temperature cooling to near 30°C downstream to reproduce the kind of gradient to be expected as off-ridge hydrothermal solutions infuse the base of the mound. After 290 mL of the hydrothermal fluid (pH 12.0) was passed through the reactor barrel for the first 24 hours, the mildly acidic ocean simulant (pH 5.3) was introduced in equal and alternating measure, switching from vessel A to vessel B.

Almost immediately upon introduction of the hydrogen gas, at the specified 100 bar pressure, the hydrothermal vent solution began flowing into the sample acquisition bottles previously purged with helium. For the first 48 hours, samples were taken at 1-hour intervals. Over the remaining experimental time, samples were taken at intervals of several hours. The hydrothermal vent solution sample containers were stored at 4°C prior to processing. Approximately 3 μ L/s of hydrothermal vent solution samples were acquired and subsequently analyzed for pH and elemental composition by a Thermo Scientific, iCAP 6300a inductively coupled plasma optical emission spectrometer (ICP-OES). The hydrothermal vent reactor was disassembled at the end of the experiment, and layers of rock wool and sulfides were immediately separated and stored at 4°C in crimp-top vials purged with helium. The helium minimizes alteration prior to imaging and analysis by environmental scanning electron microscopy (ESEM).

2.3. Operation and experimental test

As a first test of the reactor as well as a test of one aspect of the alkaline-hydrothermal hypothesis, we investigated whether anionic hydrogen sulfide (HS⁻) could be dissolved from iron monosulfide and transported in the hot alkaline solution of the chemistry we predicted for such a system. Thus, the reactor was used to simulate the effect of passing the hydrothermal fluid through sulfides in veins or pods under the seafloor with the expectation that the resulting solution would contain dissolved sulfide (Fig. 1). We also expected the FeS in the lower portion of the reactor to be partly stripped of its sulfur, which would leave a patina of ferrous hydroxide. Further up in the cooler portion of the reactor, we expected white and green rust [*i.e.*,

Fe(OH)₂ or \sim Fe₄^{II}Fe₂^{III}(OH)₁₂CO₃(H₂O)₂] and metal sulfides to precipitate on the rock wool where they might have a role as potential catalysts (Russell and Hall, 2006).



Here, we have assumed (and adopted) temperatures of up to $\sim 130^\circ\text{C}$ based on (i) the hydrogen isotopic analyses of Lost City effluent (Proskurowski *et al.*, 2006), (ii) the absence of evidence for higher temperatures in land-based alkaline (pH ≤ 12.4) hydrothermal systems in ultramafic rocks (Fallick *et al.*, 1991; Zedef *et al.*, 2000), and (iii) the highest temperature of fluids recorded at Lost City (94°C) and ESKJALDAMUR (79°C). A pressure limited to 100 bars for reasons of safety only corresponds to an overall hydrostatic depth of a kilometer, so the reactor only has the capacity to reproduce conditions to be expected where the most ancient ocean was relatively shallow. It falls short of addressing the very high pressures expected at the bottom of Europa's ocean (Vance *et al.*, 2007).

2.4. Investigation of precipitates

To investigate the effects of injecting the effluent emanating from the hydrothermal reactor into a simulacrum of the Hadean Ocean water, a batch collected after 5 hours was introduced through a 0.5 mm hole at the bottom of an inverted glass bottle into a mildly acidic solution that contained 10 mM/L ferrous iron (Russell and Hall, 2006). Two injection rates were employed, the first at 7.2 mL/hour and the second at 0.04 mL/hour. The time from removal of the precipitated structures from the aqueous solution to their placement in the freeze-drier was about 2 min. A portion of the precipitate was attached to a specimen stub by means of a carbon tab. ESEM was used to investigate the resulting structures precipitated during the experiments.

3. Results

3.1. Solution chemistry

An arresting result was the immediate conversion of the acidic ocean water to a highly alkaline solution through the dissolution of Ca from the pristine rock wool (Fig. 3). Also, a surge of hydrogen sulfide ion (as HS⁻) began about 4 hours after the beginning of operations and peaked at 460 ppm (≤ 14 mM/L) at around 6 hours as measured by ICP-OES (Fig. 3). Sulfide concentrations of 330 ppm (10 mM/L) or more were maintained for ~ 100 min during interaction with the hydrothermal solution before dropping to ~ 50 ppm (1.5 mM/L) at 12 hours and oscillated around 25–50 ppm (~ 1 mM/L) thereafter until the heaters were switched off after 9 days. Calcium also surged with the sulfide, *though to a lesser degree*. Calcium concentrations also then dropped, perhaps as a result of calcite precipitation in the upper section of the reactor where the fluids became more alkaline (Figs. 3 and 4C). Silicon concentrations correlated inversely with calcium and increased more slowly than sulfide to reach a constant 50 ppm (2 mM/L) after 2 days (Fig. 3). Iron, as expected from its minimal solubility in alkaline solution, was constantly below the detection limit of 0.1 ppm.

The delivery of calcium in the hydrothermal solution is mirrored by the alteration of the basalt rock wool that is shown prior to reaction (Fig. 4A) and after reaction (Fig. 4B).

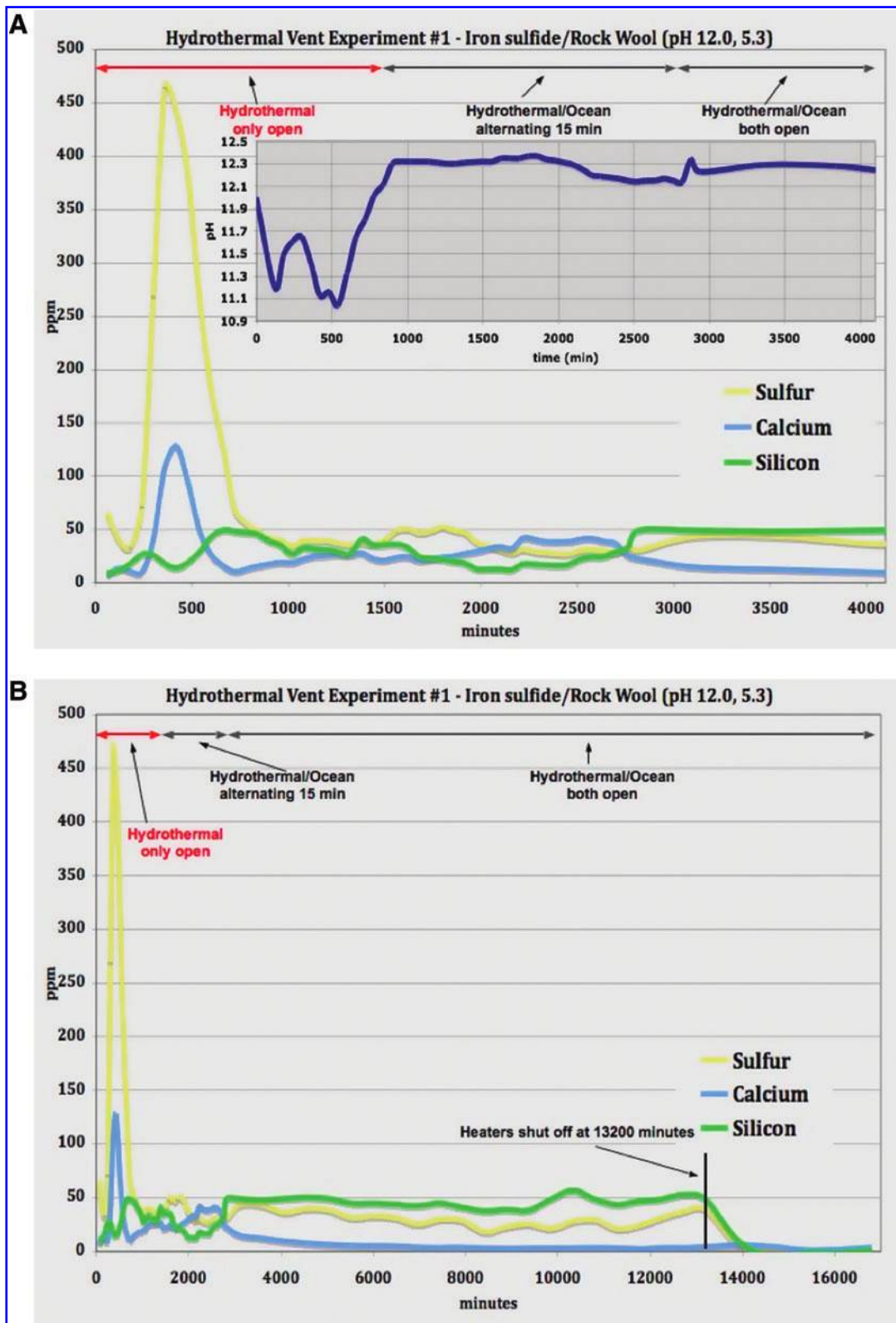


FIG. 3. Inductively coupled plasma optical emission spectrometry analysis of effluent for the time-dependent samples. Graph 3A shows the results of 60 samples collected over the first 4000 min, and graph 3B shows the complete experimental time period (250 samples). The initial few samples contained over 50 ppm of sulfur determined to be sulfate ions that dropped to zero after 240 min. Initially the pH of the hydrothermal solution dropped almost one unit before rising again after 10 hours to stabilize around pH 12.3. The operating reactor temperature was reached within 120 min, whereas the maximum sulfur concentration (as HS^-) was reached at 360 min, indicating that major dissolution of sulfide occurs only after the operating temperature is reached. The hydrothermal solution was open to the reactor for the first 1440 min followed by alternating ocean/hydrothermal solutions opened every 15 min for another 1440 min. For the remainder of the experiment both solutions were opened to the reactor. The heaters were shut off at 13,200 min, and the system was at ambient temperature by 14,000 min. At this time the concentrations of sulfur, calcium, silicon, potassium, and magnesium were below the detection limits. Color images available online at www.liebertonline.com/ast.

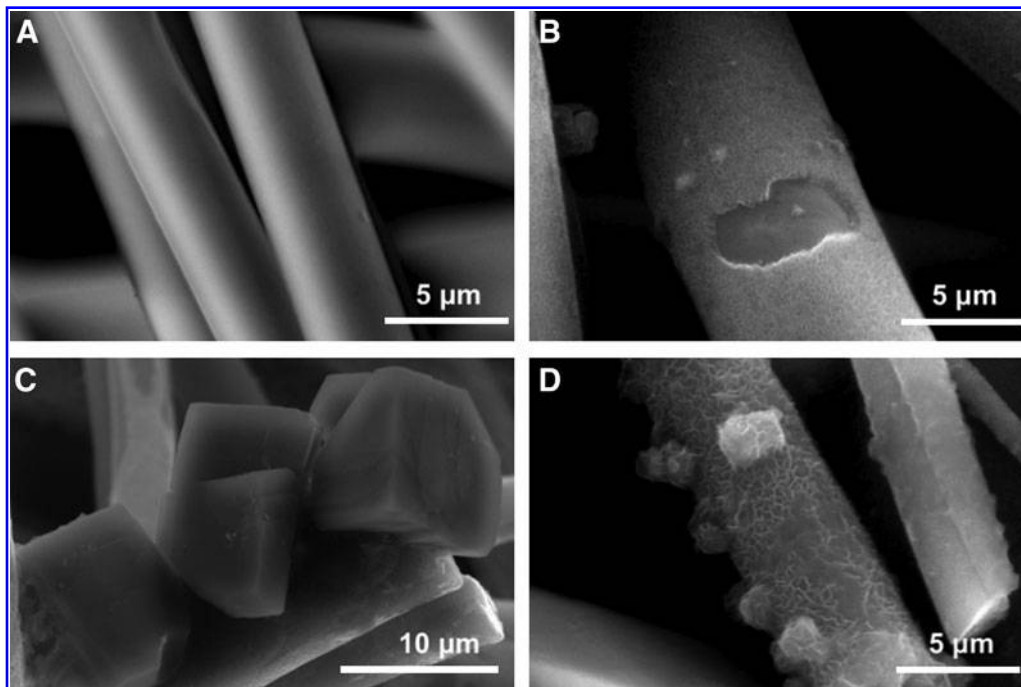


FIG. 4. (A) Environmental scanning electron microscope image of basalt rock wool prior to alteration; (B) the same rock wool comprising Layer 1, the image revealing severe surface alteration and loss of calcium (*cf.* Fig. 5). (C) Calcite precipitate on basalt rock wool from Layers 1–3. (D) Clumps of iron- and sulfide-rich minerals cover portions of the basalt rock wool of Layer 15, demonstrating local mobility of these two elements.

Figure 4C demonstrates the direct re-precipitation of calcium as the carbonate upon rock wool in the hottest, lowest section of the reactor. The dissolution of calcium from the rock wool in the hottest section of the reactor as analyzed by environmental scanning electron microscopy–energy dispersive X-ray spectroscopy (ESEM-EDX) is particularly notable (Fig. 5, 6).

3.2. Mineralogy

The basaltic rock wool and sulfides were investigated with an environmental scanning electron microscope prior to, and following, the experiment. Precipitates on the rock wool in the lower layers in the reactor consisted of calcite, whereas clumps of iron- and sulfide-rich minerals were seen to cover

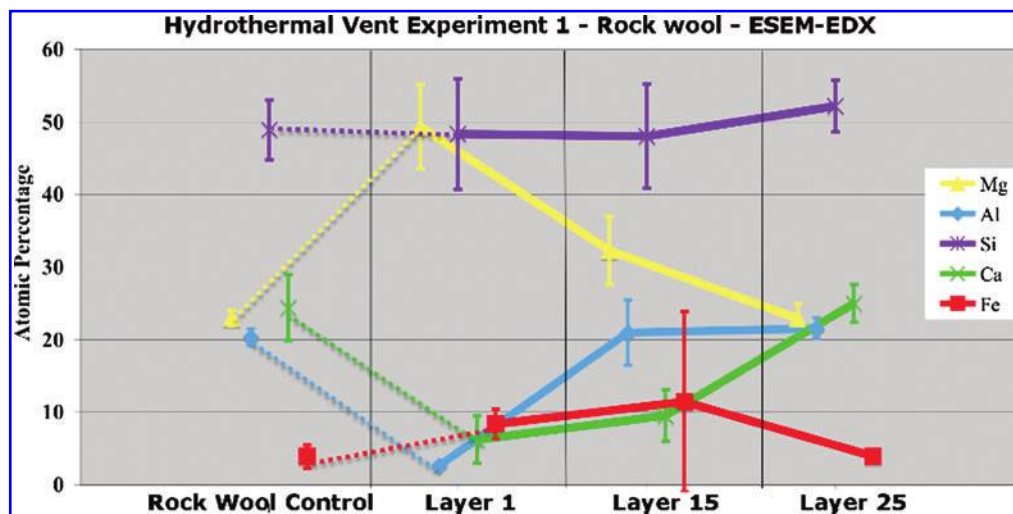


FIG. 5. The graph shows the ESEM-EDX analyses of several of the basalt rock wool layers and the basalt rock wool control ($n = 50$). The most drastic changes occurred in the amount of calcium dissolved from the surface material at the bottom of the reactor (Layer 1, $n = 44$) and in the hot zone above the iron sulfide layer (Layer 15, $n = 67$). Aluminum was also removed from Layer 1. In contrast, the top, cool portion of the reactor (Layer 25, $n = 50$) shows surface atomic ratio composition at levels equivalent to the control basalt rock wool, except for a slight enrichment of silicon. However, some of the calcium now resides in a carbonate phase in Layer 25. Color images available online at www.liebertonline.com/ast.

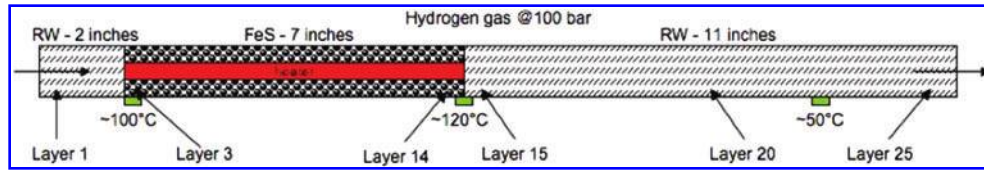


FIG. 6. Sketch of hydrothermal reactor with range of atomic S:Fe ratios on the surface of altered FeS as analyzed by ESEM (numbers of analyses in parentheses): Pristine FeS = 1.07, $1\sigma \pm 0.17$; Layer 3 = 0.50–0.21, $1\sigma \pm 0.17$ (2); Layer 6 = 0.71–0.21, $1\sigma \pm 0.19$ (3); Layer 9 = 0.42–0.33, $1\sigma \pm 0.21$ (2); Layer 12 = 0.83–0.15, $1\sigma \pm 0.19$ (5); Layer 14 = 0.62–0.01, $1\sigma \pm 0.18$ (6). Color images available online at www.liebertonline.com/ast.

portions of the rock wool high up in the reactor (Layer 15) (Figs. 4D and 7). ESEM-EDX analyses of the rock wool revealed a significant loss of calcium from the rock wool surface material at the bottom of the reactor (Layer 1, $n = 44$) as well as in the hot zone above the iron sulfide layer (Layer 15, $n = 67$) (Figs. 4B and 5). Aluminum was also lost from Layer 1. The rock wool comprising the highest, coolest level of the reactor (Layer 25, $n = 50$) was largely unaffected beyond a slight enrichment of silicon. The main change here was in the addition of calcium as calcite in Layer 25.

Iron-rich mineral overgrowth on the iron sulfide surface exhibited low to very low S:Fe ratios; values decayed from 0.94 in the relatively unaltered sulfide to ~ 0.2 , which reflects the insolubility of the iron while sulfide was lost to the alkaline solution (Fig. 6). The overgrowths were probably a form of green rust. Aluminosilicate crystals (possibly vermiculite) also occurred sparsely in the iron sulfide layers, revealing minor aluminum transport.

3.3. Chimney and geodic growth

By taking the solution eluted from the hydrothermal experiment, which contained several millimoles per liter of sulfide, and injecting it from below and into inverted glass bottles of simulated, mildly acidic ferric chloride-bearing Hadean Ocean water (pH ~ 5.3 and 10 mM FeCl_2), we found chimney morphology to be dependent on injection rate. At a rate of 7.2 mL/hour, a fibrous hollow chimney morphology was produced that had affinities to chemical garden structures (Russell and Hall, 2006) (Fig. 8A). Structures produced during low injection rates (0.04 mL/hour), as illustrated in Figs. 8B and 9, were bulbous and contained similar geodic structures within them at a much smaller scale (Russell *et al.*, 1994). The geodes and chimneys comprised an outer wall of iron hydroxide, silicate, carbonate and sulfide, and a hollow interior containing a collection of smaller well-defined geodes. One of these micro-geodes

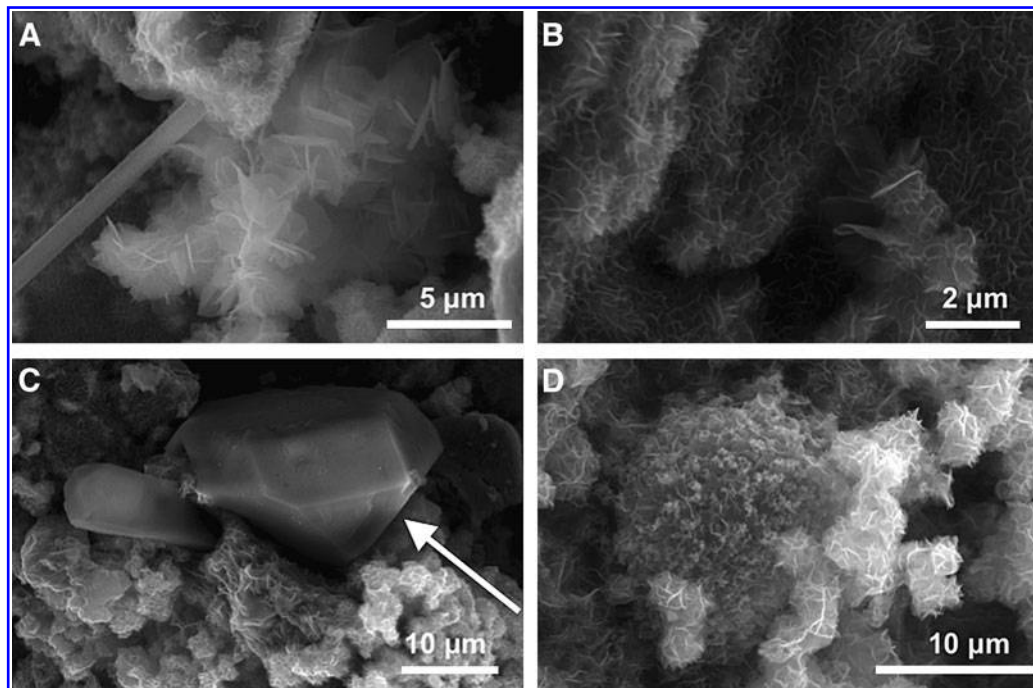


FIG. 7. Photomicrographs demonstrating the iron-rich minerals (probably green rust) precipitated on the surfaces of the iron sulfide. The S:Fe ratios of these minerals were invariably less than 1, and in many cases much less, as to be expected as sulfide was lost to solution (Fig. 3). Images (A) and (B) are from Layer 3 and show various sizes of flakey ball structures. There were other larger aluminosilicate crystals present in the iron sulfide layers (arrow) as shown in image (C). Image (D) is from Layer 14 with similar characteristic morphologies but had the largest diversity and included phases with aluminum:silicon ratio close to ~ 2 (possibly vermiculite) and only minor iron content.

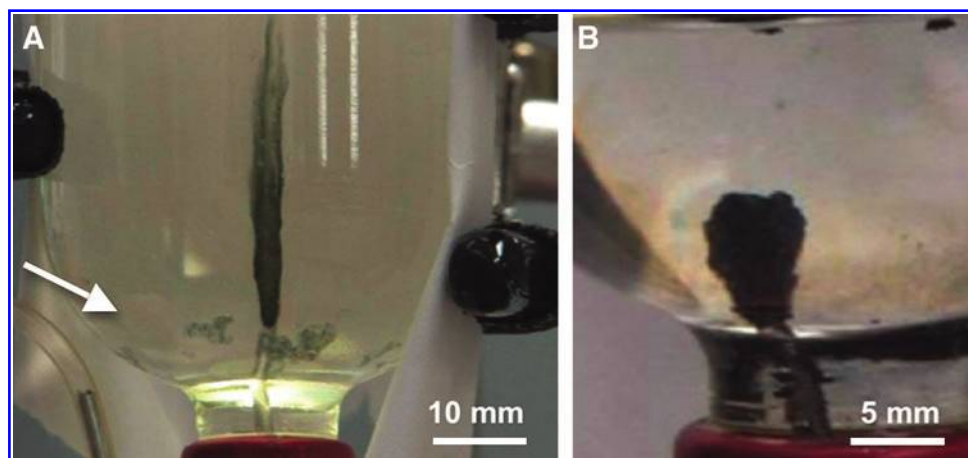


FIG. 8. Injection of the reactor effluent taken after 5 hours (Fig. 3) into the simulacrum of the Hadean Ocean containing 10 mM/L ferrous iron. When injection rate is rapid, a chimney grows to ~ 35 mm in 8 min before the top spills off and settles (white arrow) (A). Geodic growth is favored when injection rate is slow [pictured after 12 hours in (B) and detailed in Fig. 9]. Color images available online at www.liebertonline.com/ast.

was partly filled with iron-bearing nanocrysts (*cf.* Fig. 1 and Larter *et al.*, 1981, plate 2).

4. Discussion

Conditions throughout the operation of the reactor were easy to control, and the first experiment, apart from being a technical success, delivered useful data on the likely evolution of hydrothermal fluids in conditions we imagine for early Earth. The delivery rate of effluent from the reactor was limited to ~ 0.2 mL/min. As might be expected, the

simulacrum of the acidic ocean water was rendered highly alkaline as it traversed the basalt rock wool at temperatures at or below 130°C (Macleod *et al.*, 1994). In fact, the pH oscillated between 11 and 12.3 as measured at standard temperature and pressure regardless of the pH of the introduced solution. This is the kind of pH met with in many cool to warm springs operating in ultramafic oceanic rocks, and pH values of up to 12.5 have been recorded in pore waters in serpentinite seamounts at a depth of 4 km in the Southern Mariana Forearc (Salisbury, 2002). Nevertheless, chrysotile asbestos wool would obviously furnish a more

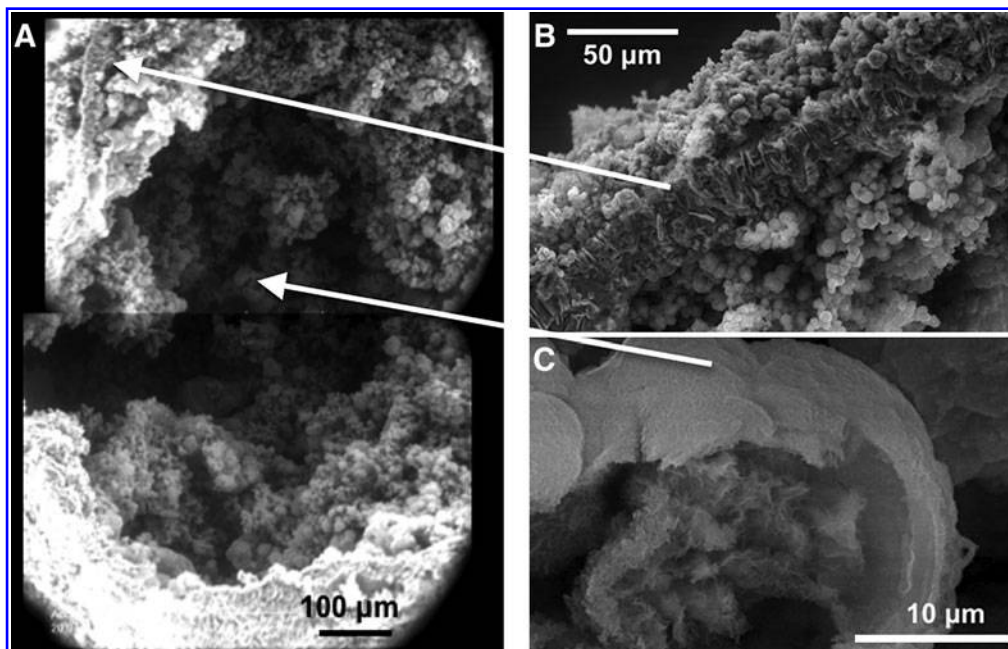


FIG. 9. Environmental scanning electron microscope images of a cross section near the base of the inflated geode figured in 8B shown to comprise an outer mixed iron hydroxide, silicate, carbonate, and sulfide wall (A and B) and a hollow interior containing a collection of smaller well-defined geodes. One of these microgeodes is revealed as partly filled with fluffy nanocrysts of iron-bearing minerals (C). Compare with Fig. 1.

realistic substrate than the rock wool used in this experiment, but it was precluded for reasons of health and safety. Calcium, generally oscillating around 25 ppm and partly responsible for the high pH, appears to have been leached out of the rock wool after 27 hours or was reprecipitating higher in the reactor (Figs. 3 and 4).

At a peak of 14 mM/L, sulfide concentrations approached the theoretical maxima calculated for alkaline hydrothermal solutions (Macleod *et al.*, 1994, p 36), before falling back to around 1 mM/L. Even at this level, the concentration is quite enough to ensure some sulfide precipitation in a putative hydrothermal mound. The sulfur values correlate positively with calcium and negatively with pH and silicon. The concentration of silica approaches 2 mM/L, which is to be expected in such alkaline hydrothermal solutions where there is a source of free silica (Marteinsson *et al.*, 2001). Thereafter, sulfur values oscillate between 1 and 2 mM/L and silica between 0.5 and 2 mM/L. Why there should be a peak concentration of 14 mmol/kg of hydrogen sulfide ion around 6 hours is puzzling and could be the result of the dissolution of free sulfur from the commercial FeS used here. However, these results speak against the possibility that the first compartments of life consisted purely of sulfides (*cf.* Russell *et al.*, 1994). Nevertheless, there would be enough sulfide to ensure a component of (catalytic) iron-nickel-cobalt sulfide within the walls of compartments that otherwise would be composed of carbonate, green rust, silicates, or silica itself. Indeed, an effluent solution sample taken from the reactor after 5 hours was introduced through the base of inverted glass bottles into a ferrous chloride solution that simulated the heavy metal-rich Hadean Ocean, and a complex of chimneys and geodes were produced as expected, which consisted mainly of silica or silicate, ferrous hydroxide, and minor sulfide (Fig. 9A, 9B). At the high pH conditions maintained by the reacted fluid, a major stable phase for iron in the chimneys was probably white or green rust [$\sim \text{Fe}(\text{OH})_2$], as indicated by the ESEM-EDX analysis, though with scattered ferrous sulfide (Fig. 7A). Such transition-metal sulfide catalysts would thereby be ripe for participation in the growing network of reactions requisite for the onset of metabolism (McGlynn *et al.*, 2009; Berg *et al.*, 2010; Haydon *et al.*, 2010; Say and Fuchs, 2010).

Both types of hollow structure may have been significant in the emergence of life. The microgeodes may have harbored the simple organic molecules synthesized through the hydrogenation of carbon dioxide as CO_2 seeped through the inorganic walls to the chambers where it met H_2 on the catalytic sulfides that comprised portions of the interior—a focus for our future experiments. The energy to drive the hydrogenation could have been supplied by an ambient chemiosmotic gradient that acted across the inorganic membrane via suitable variable valence metal catalysts (Nitschke and Russell, 2009; Lane *et al.*, 2010). At a more advanced state of metabolic evolution, the thin cylindrical structures might have supported a convective polymerase chain reaction and a thermal diffusive concentration reaction of charged polymers such as RNA (Baaske *et al.*, 2007; Mast and Braun, 2010). We suggest that it is in such inhibiting circumstances that life would have emerged.

We envisage the next experimental step as using the reactor in an attempt to synthesize methane and other organic

intermediates while an alkaline hydrothermal solution that bears sulfide and hydrogen, as well as molybdenum and tungsten ions, is introduced to a simulacrum of the early ocean that bears carbon dioxide, ferrous iron, and minor nickel in solution. In these future experiments, natural sulfide minerals will be introduced to, or precipitated in, the reactor; and a safe protocol to use fibrous serpentinite minerals as packing and substrate will be developed. Carbon dioxide will be introduced to the ocean simulacrum to investigate the power of the system to reduce this gas, as occurs in the Lost City serpentinizing system (Proskurowski *et al.*, 2008; Konn *et al.*, 2009).

Acknowledgments

We thank Lawrence Wade for help with fabrication; Grazyna Orzechowska for support; and Bill Martin, Steven Vance, and Hreiðar Þór Valtýsson for discussions. Anonymous referees gave helpful critiques. S.E.M. was supported by the Marine Biological Laboratories NASA Planetary Biology Internship Program and acknowledges support by a NSF IGERT Fellowship by the MSU Program in Geobiological Systems (DGE 0654336). The research described in this publication was carried out at the Jet Propulsion Laboratory, California Institute of Technology, under a contract with the National Aeronautics and Space Administration: with initial support by JPL grant (R.06.021.071) and subsequently by NASA Exobiology and Evolutionary Biology award (NNH06ZDA001N) and supported by the NASA Astrobiology Institute (Icy Worlds).

Disclosure Statement

There are no competing interests.

Abbreviations

EDX, energy dispersive X-ray spectroscopy; ESEM, environmental scanning electron microscopy; ICP-OES, inductively coupled plasma optical emission spectrometer.

References

- Abrajano, T.A., Sturchio, N.C., Kennedy, B.M., Lyon, G.L., Muehlenbachs, K., and Bohlke, J.K. (1990) Geochemistry of reduced gas related to serpentinization of the Zambales ophiolite, Philippines. *Appl Geochem* 5:625–630.
- Allen, D.E. and Seyfried, W.E. (2004) Serpentinization and heat generation: constraints from Lost City and Rainbow hydrothermal systems. *Geochim Cosmochim Acta* 68:1347–1354.
- Baaske, P., Weinert, F., Duhr, S., Lemke, K., Russell, M.J., and Braun, D. (2007) Extreme accumulation of nucleotides in simulated hydrothermal pore systems. *Proc Natl Acad Sci USA* 104:9346–9351.
- Barnes, I., Rapp, J.B., and O'Neil, J.R. (1972) Metamorphic assemblages and the direction of flow of metamorphic fluids in four instances of serpentinization. *Contrib Mineral Petrol* 35:263–276.
- Berg, I.A., Kockelkorn, D., Ramos-Vera, W.H., Say, R.F., Zarzycki, J., Hügler, M., Alber, B.E., and Fuchs, G. (2010) Autotrophic carbon fixation in archaea. *Nat Rev Microbiol* 8:447–460.
- Bonatti, E., Simmons, E.C., Breger, D., Hamlyn, P.R., and Lawrence, J. (1983) Ultramafic rock/seawater interaction in the oceanic crust: Mg-silicate (sepiolite) deposit from the Indian Ocean floor. *Earth Planet Sci Lett* 62:229–238.

- Braterman, P.S., Cairns-Smith, A.G., and Sloper, R.A. (1983) Photo-oxidation of hydrated Fe^{2+} —significance for banded iron formations. *Nature* 303:163–164.
- Charlou, J.L., Donval, J.P., Konn, C., Ondreas, H., Fouquet, Y., Jean-Baptiste, P., and Fourré, E. (2010) High production and fluxes of H_2 and CH_4 and evidence of abiotic hydrocarbon synthesis by serpentinization in ultramafic-hosted hydrothermal systems on the Mid-Atlantic Ridge. In *Diversity of Hydrothermal Systems on Slow Spreading Ocean Ridges*, edited by P. Rona, C. Devey, J. Dymont, and B. Murton, AGU Geophysical Monograph 188, American Geophysical Union, Washington DC.
- Corliss, J.B. (1986) On the creation of living cells in submarine hot spring flow reactors: attractors and bifurcations in the natural hierarchy dissipative systems. *Orig Life Evol Biosph* 19:381–382.
- Delacour, A., Früh-Green, G.L., and Bernasconi, S.M. (2008) Sulfur mineralogy and geochemistry of serpentinites and gabbros of the Atlantis Massif (IODP Site U1309). *Geochim Cosmochim Acta* 72:5111–5127.
- Douville, E., Charlou, J.L., Oelkers, E.H., Bienvenu, P., Colon, C.F.J., Donval, J.P., Fouquet, Y., Prieur, D., and Appriou, P. (2002) The rainbow vent fluids (36°14'N, MAR): the influence of ultramafic rocks and phase separation on trace metal content in Mid-Atlantic Ridge hydrothermal fluids. *Chem Geol* 184:37–48.
- Emmanuel, S. and Berkowitz, B. (2006) Suppression and stimulation of seafloor hydrothermal convection by exothermic mineral hydration. *Earth Planet Sci Lett* 243:657–668.
- Fallick, A.E., Ilich, M., and Russell, M.J. (1991) A stable isotope study of the magnesite deposits associated with the Alpine-type ultramafic rocks of Yugoslavia. *Econ Geol* 86:847–861.
- Foustoukos, D.I., Savov, I.P., and Janecky, D.R. (2008) Chemical and isotopic constraints on water/rock interactions at the Lost City hydrothermal field, 30°N Mid-Atlantic Ridge. *Geochim Cosmochim Acta* 72:5457–5474.
- Gautason, B., Valtysson, H.T., Einarsson, H., Eythorsdóttir, A., Bogason, E., and Steingrímsson, S.A. (2005) Arnarnesstrytur: a recently discovered active shallow marine hydrothermal system in Eyjafjörður, Iceland [abstract OS21C-02]. In *Eos Transactions AGU*, Vol. 86, Fall Meeting Supplement, American Geophysical Union, Washington DC.
- Hand, K.P., Carlson, R.W., and Chyba, C.F. (2007) Energy, chemical disequilibrium, and geological constraints on Europa. *Astrobiology* 7:1006–1022.
- Hand, K.P., Chyba, C.F., Priscu, J.C., Carlson, R.W., and Nealson, K.H. (2010) Astrobiology and the potential for life on Europa. In *Europa*, edited by R. Pappalardo, W. McKinnon, and K. Khurana, University of Arizona Press, Tucson, AZ, pp 589–629.
- Haydon, N., McGlynn, S.E., and Robus, O. (2010) Speculation on quantum mechanics and the operation of life giving catalysts. *Orig Life Evol Biosph* doi:10.1007/s11084-010-9210-5.
- Kehew, A.E. (2001) *Applied Chemical Hydrogeology*, Prentice-Hall, Upper Saddle River, NJ.
- Kelley, D.S., Karson, J.A., Blackman, D.K., Früh-Green, G.L., Butterfield, D.A., Lilley, M.D., Olsen, E.J., Schrenk, M.O., Roe, K.K., Lebon, G.T., Rivizzigno, P., and the AT3-60 Shipboard Party. (2001) An off-axis hydrothermal vent field near the Mid-Atlantic Ridge at 30°N. *Nature* 412:145–149.
- Kelley, D.S., Karson, J.A., Früh-Green, G.L., Yoerger, D.R., Shank, T.M., Butterfield, D.A., Hayes, J.M., Schrenk, M.O., Olson, E.J., Proskurowski, G., Jakuba, M., Bradley, A., Larson, B., Ludwig, K., Glickson, D., Buckman, K., Bradley, A.S., Brazelton, W.J., Roe, K., Elend, M.J., Delacour, A., Bernasconi, S.M., Lilley, M.D., Baross, J.A., Summons, R.E., and Sylva, S.P. (2005) A serpentinite-hosted ecosystem: the Lost City hydrothermal field. *Science* 307:1428–1434.
- Knauth, L.P. and Lowe, D.R. (2003) High Archean climatic temperature inferred from oxygen isotope geochemistry of cherts in the 3.5 Ga Swaziland Supergroup, South Africa. *Geol Soc Am Bull* 115:566–580.
- Konn, C., Charlou, J.L., Donval, J.P., Holm, N.G., Dehairs, F., and Bouillon, S. (2009) Hydrocarbons and oxidized organic compounds in hydrothermal fluids from Rainbow and Lost City ultramafic-hosted vents. *Chem Geol* 258:299–314.
- Kump, L.R. and Seyfried, W.E. (2005) Hydrothermal Fe fluxes during the Precambrian: effect of low oceanic sulfate concentrations and low hydrostatic pressure on the composition of black smokers. *Earth Planet Sci Lett* 235:654–662.
- Lane, N., Allen, J.F., and Martin W. (2010) How did LUCA make a living? Chemiosmosis in the origin of life. *Bioessays* 32:271–280.
- Larter, R.C.L., Boyce, A.J., and Russell, M.J. (1981) Hydrothermal pyrite chimneys from the Ballynoe baryte deposit, Silvermines, County Tipperary, Ireland. *Mineralium Deposita* 16:309–318.
- Leshner, C.M. and Stone, W.E. (1997) Exploration geochemistry of komatiites. In *Trace Element Geochemistry of Volcanic Rocks: Applications for Massive Sulphide Exploration*, Short Course Notes Vol. 12, edited by D.A. Wyman, Geological Society of Canada, St. John's, Canada, pp 153–204.
- Lowell, R.P. and Rona, P.A. (2002) Seafloor hydrothermal systems driven by the serpentinization of peridotite. *Geophys Res Lett* 29, doi:10.1029/2001GL014411.
- Ludwig, K.A., Kelley, D.S., Shen, C., Cheng, H., and Edwards, R.L. (2005) U/Th geochronology of carbonate chimneys at the Lost City hydrothermal field [abstract V51B-1487]. In *Eos Transactions AGU*, Vol. 86, Fall Meeting Supplement, American Geophysical Union, Washington DC.
- Macleod, G., McKeown, C., Hall, A.J., and Russell, M.J. (1994) Hydrothermal and oceanic pH conditions of possible relevance to the origin of life. *Orig Life Evol Biosph* 24:19–41.
- Marteinson, V.Th., Kristjánsson, J.K., Kristmannsdóttir, H., Dahlkvist, M., Sæmundsson, K., Hannington, M., Pétursdóttir, S.K., Geptner, A., and Stoffers, P. (2001) Discovery of giant submarine smectite cones on the seafloor in Eyjafjörður, Northern Iceland, and a novel thermal microbial habitat. *Appl Environ Microbiol* 67:827–833.
- Martin, W. and Russell, M.J. (2007) On the origin of biochemistry at an alkaline hydrothermal vent. *Philos Trans R Soc Lond B Biol Sci* 362:1887–1925.
- Martin, R.S., Mather, T.A., and Pyle, D.M. (2007) Volcanic emissions and the early Earth atmosphere. *Geochim Cosmochim Acta* 71:3673–3685.
- Martin, W., Baross, J., Kelley, D., and Russell, M.J. (2008) Hydrothermal vents and the origin of life. *Nat Rev Microbiol* 6:805–814.
- Mast, C.B. and Braun, D. (2010) Thermal trap for DNA replication. *Phys Rev Lett* 104:188102.
- McGlynn, S.E., Mulder, D.W., Shepard, E.M., Broderick, J.B., and Peters, J.W. (2009) Hydrogenase cluster biosynthesis: organometallic chemistry nature's way. *Dalton Trans* 2009, 4274–4285, doi:10.1039/b821432h.
- Neal, C. and Stanger, G. (1984) Calcium and magnesium hydroxide precipitation from alkaline groundwater in Oman, and their significance to the process of serpentinization. *Mineral Mag* 48:237–241.
- Nitschke, W. and Russell, M.J. (2009) Hydrothermal focusing of chemical and chemiosmotic energy, supported by delivery of

- catalytic Fe, Ni, Mo/W, Co, S and Se, forced life to emerge. *J Mol Evol* 69:481–496.
- Nitschke, W. and Russell, M.J. (2010) Just like the Universe the emergence of life had high enthalpy and low entropy beginnings. *Journal of Cosmology* 10:3200–3216.
- Palandri, J. and Reed, M.H. (2004) Geochemical models of metasomatism in ultramafic systems: serpentinization, rodingitization, and sea floor carbonate chimney precipitation. *Geochim Cosmochim Acta* 68:1115–1133.
- Proskurowski, G., Lilley, M.D., Kelley, D.S., and Olson, E.J. (2006) Low temperature volatile production at the Lost City Hydrothermal Field, evidence from a hydrogen stable isotope geothermometer. *Chem Geol* 229:331–343.
- Proskurowski, G., Lilley, M.D., Seewald, J.S., Früh-Green, G.L., Olson, E.J., Lupton, J.E., Sylva, S.P., and Kelley, D.S. (2008) Abiogenic hydrocarbon production at Lost City hydrothermal field. *Science* 319:604–607.
- Russell, M.J. (1978) Downward-excavating hydrothermal cells and Irish-type ore deposits: importance of an underlying thick Caledonian Prism. *Transactions of the Institution of Mining and Metallurgy. Section B: Applied Earth Science* 89:B168–B171.
- Russell, M.J. and Hall, A.J. (1997) The emergence of life from iron monosulphide bubbles at a submarine hydrothermal redox and pH front. *J Geol Soc London* 154:377–402.
- Russell, M.J. and Hall, A.J. (2006) The onset and early evolution of life. In *Evolution of Early Earth's Atmosphere, Hydrosphere, and Biosphere—Constraints from Ore Deposits*, Geological Society of America Memoir 198, edited by S. Kesler and H. Ohmoto, Geological Society of America, Boulder, CO, pp 1–32.
- Russell, M.J. and Martin, W. (2004) The rocky roots of the acetyl-CoA pathway. *Trends Biochem Sci* 29:358–363.
- Russell, M.J., Hall, A.J., and Turner, D. (1989) *In vitro* growth of iron sulphide chimneys: possible culture chambers for origin-of-life experiments. *Terra Nova* 1:238–241.
- Russell, M.J., Daniel, R.M., Hall, A.J., and Sherringham, J. (1994) A hydrothermally precipitated catalytic iron sulphide membrane as a first step toward life. *J Mol Evol* 39:231–243.
- Russell, M.J., Hall, A.J., and Martin, W. (2010) Serpentinization as a source of energy at the origin of life. *Geobiology* 8, doi:10.1111/j.1472-4669.2010.00249.x.
- Salisbury, M.H. (2002) Leg 195 Shipboard Scientific Party Site 1200. In *Proceedings of the Ocean Drilling Program, Initial Reports*, Vol. 195, Ocean Drilling Program, College Station, TX. Available online at http://www-odp.tamu.edu/publications/195_IR/195TOC.HTM.
- Say, R.F. and Fuchs, G. (2010) Fructose 1,6-bisphosphate aldolase/phosphatase may be an ancestral gluconeogenic enzyme. *Nature* 464:1077–1081.
- Vance, S., Harnmeijer, J., Kimura, J., Hussmann, H., Demartin, B., and Brown, J.M. (2007) Hydrothermal systems in small ocean planets. *Astrobiology* 7:987–1005.
- Wächtershäuser, G. (2006) From volcanic origins of chemoautotrophic life to Bacteria, Archaea and Eukarya. *Philos Trans R Soc Lond B Biol Sci* 361:1787–1808.
- Wetzel, L.R. and Shock, E.L. (2000) Distinguishing ultramafic-from basalt-hosted submarine hydrothermal systems by comparing calculated vent fluid compositions. *J Geophys Res* 105:8319–8340.
- Wiebe, R. and Gaddy, V.L. (1934) The solubility of hydrogen in water at 0, 50, 75 and 100° from 25 to 1000 atmospheres. *J Am Chem Soc* 56:76–79.
- Yamagata, Y., Wanatabe, H., Saitoh, M., and Namba, T. (1991) Volcanic production of polyphosphates and its relevance to prebiotic evolution. *Nature* 352:516–519.
- Zedef, V., Russell, M.J., Hall, A.J., and Fallick, A.E. (2000) Genesis of vein-stockwork and sedimentary magnesite and hydro-magnesite deposits in the ultramafic terranes of southwestern Turkey: a stable isotope study. *Econ Geol* 95:429–446.

Address correspondence to:

Michael Russell
Planetary Science
Section 3220
MS:183-301

Jet Propulsion Laboratory
California Institute of Technology
4800 Oak Grove Drive
Pasadena, CA 91109-8099
USA

E-mail: mrussell@jpl.nasa.gov

Isik Kanik
Planetary Science
Section 3220
MS:183-601

Jet Propulsion Laboratory
California Institute of Technology
4800 Oak Grove Drive
Pasadena, CA 91109-8099
USA

E-mail: isik.kanik@jpl.nasa.gov

Submitted 9 December 2009

Accepted 18 July 2010

This article has been cited by:

1. S. E. McGlynn, I. Kanik, M. J. Russell. 2012. Peptide and RNA contributions to iron-sulphur chemical gardens as life's first inorganic compartments, catalysts, capacitors and condensers. *Philosophical Transactions of the Royal Society A: Mathematical, Physical and Engineering Sciences* **370**:1969, 3007-3022. [[CrossRef](#)]
2. Nick Lane. 2012. Thermodynamics, formamide, and the origin of life. *Physics of Life Reviews* . [[CrossRef](#)]
3. H. James Cleaves II, Andrea Michalkova Scott, Frances C. Hill, Jerzy Leszczynski, Nita Sahai, Robert Hazen. 2012. Mineral–organic interfacial processes: potential roles in the origins of life. *Chemical Society Reviews* **41**:16, 5502. [[CrossRef](#)]
4. Randall E. Mielke , Kirtland J. Robinson , Lauren M. White , Shawn E. McGlynn , Kavan McEachern , Rohit Bhartia , Isik Kanik , Michael J. Russell . 2011. Iron-Sulfide-Bearing Chimneys as Potential Catalytic Energy Traps at Life's Emergence. *Astrobiology* **11**:10, 933-950. [[Abstract](#)] [[Full Text HTML](#)] [[Full Text PDF](#)] [[Full Text PDF with Links](#)]
5. Laura M. Barge, Ivria J. Doloboff, Lauren M. White, Galen D. Stucky, Michael J. Russell, Isik Kanik. 2011. Characterization of Iron–Phosphate–Silicate Chemical Garden Structures. *Langmuir* 111116111507009. [[CrossRef](#)]
6. Mohammad Mahdi Najafpour. 2011. Calcium-manganese oxides as structural and functional models for active site in oxygen evolving complex in photosystem II: Lessons from simple models. *Journal of Photochemistry and Photobiology B: Biology* **104**:1-2, 111-117. [[CrossRef](#)]